PERGAMON

International Journal of Impact Engineering 24 (2000) 545–560

INTERNATIONAL JOURNAL OF IMPACT ENGINEERING

www.elsevier.com/locate/ijimpeng

A visco-hyperelastic approach to modelling the constitutive behaviour of rubber

L.M. Yang, V.P.W. Shim*, C.T. Lim

Department of Mechanical and Production Engineering, National University of Singapore, 10 Kent Ridge Crescent, Singapore 119260, Singapore

Received 6 April 1999; received in revised form 15 July 1999; accepted 26 July 1999

Abstract

A visco-hyperelastic constitutive equation is proposed to describe the large-deformation response of incompressible rubber under high strain rates. The equation comprises two parts — a component with three parameters to characterise static hyperelastic behaviour, and another also with three parameters to define rate-sensitivity and strain history dependence. Relatively straightforward static and dynamic experimental techniques are employed to determine the six parameters in the constitutive relationship. Comparison of predictions based on the proposed model with experiments shows that it is able to aptly describe visco-hyperelastic behaviour of rubber-like materials under high strain rates. The material model is also used in a simulation of the three-dimensional dynamic response of a rubber pad to impact. Comparison with experimental results shows that there is good agreement with the simulation.

Keywords: High strain rate; Visco-hyperelasticity; Constitutive model; Rubber

1. Introduction

Rubber components are widely used for vibration isolation, in energy storage devices and as buffers between neighbouring components in products that are subjected to possible impact loads. The last application includes the accidental dropping of electronic consumer products on hard surfaces or impact with neighbouring objects. The choice of a suitable buffer or shock pad material is crucial, to achieve satisfactory protection from such damage. For effective shock amelioration, the mechanical properties of the buffer material have to be determined for a spectrum of strain

* Corresponding author.

0734-743X/00/$ - see front matter
PII: S0734-743X(99)00044-5

Nomenclature

a non-dimensionalised modelling parameter
A_i modelling parameters
B left Cauchy–Green deformation tensor
B_{ij} components of **B**
C right Cauchy–Green deformation tensor
$\dot{\mathbf{D}}$ non-dimensionalised strain rate
E Green-Lagrange strain tensor
$\dot{\mathbf{E}}$ strain rate tensor
F deformation gradient tensor
I unit tensor
I_i invariants of **B**
I'_i invariants of **C**
p pressure
s non-dimensionalised time
S non-dimensionalised stress tensor
t time
W strain energy potential
x position vector of a material particle at time t
X initial position vector of a material particle

Greek letters
β integral variable of non-dimensionalised time
ε_{ij} components of engineering strain
$\dot{\zeta}$ non-dimensionalised stretch rate
θ_i relaxation time
λ stretch
$\dot{\lambda}$ stretch rate
σ Cauchy stress tensor
σ^0_{ij} components of engineering stress
σ_{ij} components of σ
τ integral variable of time
$\mathbf{\Omega}$ constitutive functional

Superscripts
e elastic
T transposition of a tensor
η viscoelastic

rates. This investigation involves the formulation of an appropriate constitutive relationship for rubber-like materials under a wide range of strain rates (10^{-3}–$10^{3}\ s^{-1}$).

It is well known that the mechanical behaviour of rubber-like materials is rate-dependent [1,2]. The works of Ward [3] and Drozdov [4] contain an introduction to a number of methods to describe rate-dependent behaviour. However, experimental data pertaining to rubber-like materials are almost entirely focused on creep, relaxation or deformation at very low strain rates ($< 10^{0}\ s^{-1}$). The accompanying analyses consequently also concentrate on low strain rate response. Viscoelastic behaviour under high strain rates such as impact loading, has received relatively little attention, possibly the result of difficulties in high rate, large deformation testing. Dynamic tests are often effected using Split Hopkinson Pressure Bar (SHPB) equipment. In general, rubber is rather compliant; therefore, the stress transmitted to the output bar is too small to be detected by normal SHPB devices. In the present study, this limitation is overcome by using polycarbonate bars in place of metal ones normally associated with Hopkinson Bar devices [5]. The mechanical impedance of polycarbonate pressure bars is much closer to that of the rubber specimens. Thus, the transmitted wave is sufficiently large for measurement. Experimental data for rubber-like materials in the present study shows that stress values obtained under high strain rates are much larger than those at low strain rates, for a given strain state. Specimens essentially regain their original geometry after unloading and residual strains are negligible, even when the maximum engineering strain induced is larger than 0.5. This indicates that the behaviour observed is amenable to description by a visco-hyperelastic material model.

In this paper, a static hyperelastic constitutive equation for rubber-like materials is first considered, followed by examination of a viscoelastic constitutive model. The two are then combined to yield a visco-hyperelastic constitutive relationship for rubber-like materials loaded at high strain rates. The proposed model is then used in the simulation of a three-dimensional impact situation to confirm its applicability.

2. Hyperelasticity

Consider a point initially located at some position $\mathbf{X}$ in a material. Displacement to a new position $\mathbf{x}$ after deformation results in a deformation gradient $\mathbf{F}$ defined by: $\mathbf{F} = \partial\mathbf{x}/\partial\mathbf{X}$. Deformation of the material can be described by the left Cauchy–Green deformation tensor $\mathbf{B}(= \mathbf{F}\cdot\mathbf{F}^{\mathrm{T}})$, or by the right Cauchy–Green deformation tensor $\mathbf{C}(= \mathbf{F}^{\mathrm{T}}\cdot\mathbf{F})$ which is related to the Green strain tensor $\mathbf{E} = (\mathbf{C} - \mathbf{I})/2$. The three invariants of $\mathbf{B}$ are defined by: $I_1 = \mathrm{tr}(\mathbf{B})$, $I_2 = [I_1^2 - \mathrm{tr}(\mathbf{B}^2)]/2$ and $I_3 = \det(\mathbf{B})$. It is reasonable to assume that rubber-like materials are incompressible, which results in $I_3 = 1$.

Following the analysis of Rivlin [6], constitutive relations for an isotropic incompressible hyperelastic material can be expressed as

$$\sigma^{\mathrm{e}} = -p_{\mathrm{e}}\mathbf{I} + \alpha_1\mathbf{B} + \alpha_2\mathbf{B}\cdot\mathbf{B}, \tag{1}$$

where p_{e} is the pressure, $\alpha_1 = 2(\partial W/\partial I_1 + I_1\partial W/\partial I_2)$, $\alpha_2 = -2\partial W/\partial I_2$ and σ^{e} is the Cauchy stress tensor. $W = W(I_1, I_2)$ is a strain energy potential which is assumed to be representable by a polynomial series involving $(I_1 - 3)$ and $(I_2 - 3)$. Brown [7] has discussed how the number of terms in W affects the resulting stress–strain curves. Based on his analysis and present quasi-static

experiments which show that the stress increases rapidly when the strain becomes large, three terms in the polynomial series are sufficient to fit the test data; i.e.

$$W = A_1(I_1 - 3) + A_2(I_2 - 3) + A_3(I_1 - 3)(I_2 - 3), \tag{2}$$

where A_1, A_2 and A_3 are parameters determined via one-dimensional tests. Consider uniaxial loading of a specimen. The stretch in the loading direction is denoted by λ; hence, the principal stretches are $\lambda_1 = \lambda$, $\lambda_2 = \lambda_3 = \lambda^{-1/2}$. The resulting deformation gradient $\mathbf{F}$ and the left Cauchy–Green deformation tensor $\mathbf{B}$ (for uniaxial loading, $\mathbf{B} = \mathbf{C}$) are

$$\mathbf{F} = \begin{bmatrix} \lambda & 0 & 0 \\ 0 & \lambda^{-1/2} & 0 \\ 0 & 0 & \lambda^{-1/2} \end{bmatrix}, \quad \mathbf{B} = \mathbf{F} \cdot \mathbf{F}^{\mathrm{T}} = \begin{bmatrix} \lambda^2 & 0 & 0 \\ 0 & \lambda^{-1} & 0 \\ 0 & 0 & \lambda^{-1} \end{bmatrix}. \tag{3}$$

The invariants are therefore

$$I_1 = \mathrm{tr}(\mathbf{B}) = \lambda^2 + 2\lambda^{-1}, \quad I_2 = \tfrac{1}{2}[I_1^2 - \mathrm{tr}(\mathbf{B}^2)] = \lambda^{-2} + 2\lambda. \tag{4}$$

From Eqs. (1) and (2), the expression for stress under uniaxial loading is

$$\sigma_{11}^{\mathrm{e}} = -p_{\mathrm{e}} + \alpha_1 B_{11} + \alpha_2 B_{11}^2, \tag{5}$$

where

$$\alpha_1 = 2[A_1 + A_2 I_1 + A_3(I_1^2 - 3I_1 + I_2 - 3)], \quad \alpha_2 = -2[A_2 + A_3(I_1 - 3)] \tag{6}$$

and σ_{11}^{e} is the Cauchy (true) stress. (The engineering stress σ_{11}^0 is related to the true stress by $\sigma_{11}^{\mathrm{e}} = \lambda\sigma_{11}^0$.) The hydrostatic pressure p_{e} is obtained from the condition $\sigma_{22}^{\mathrm{e}} = \sigma_{33}^{\mathrm{e}} = 0$, together with the relation $B_{22} = B_{11}^{-1/2}$:

$$\sigma_{22}^{\mathrm{e}} = 0 = -p_{\mathrm{e}} + \alpha_1 B_{11}^{-1/2} + \alpha_2 B_{11}^{-1}. \tag{7}$$

The constitutive relationship is applied to one-dimensional loading by combining Eqs. (6) and (7), and this can be written as a function of the stretch λ,

$$\sigma_{11}^{\mathrm{e}} = 2\lambda(1 - \lambda^{-3})\{A_1\lambda + A_2 + A_3[I_1 - 3 + \lambda(I_2 - 3)]\}. \tag{8}$$

The relationship between stretch λ and engineering strain ε_{11} in the direction of the uniaxially applied load is $\lambda = 1 + \varepsilon_{11}$. Quasi-static compression tests, at a strain rate of $0.001\ \mathrm{s}^{-1}$, were conducted on rubber specimens of two hardnesses (SHA30 and SHA70) and Eq. (8) was used to fit the experimental data using a simple least-squares approach. Values of the parameters A_1, A_2 and A_3 for the two materials are presented in Table 1. In ascertaining these parameters, it was assumed that at low strain rates, the material response is essentially rate-independent. Comparisons between empirical curves, relating true stress to engineering strain, and test data are shown in Fig. 1, which shows good correlation with experimental data for both materials. This substantiates the validity of the proposed hyperelastic constitutive model for soft (SHA30) and stiff (SHA70) rubber-like materials.

Table 1
Parameters in proposed stress–strain equation

Material	A_1 (MPa)	A_2 (MPa)	A_3 (MPa)	A_4 (MPa)	A_5 (MPa)	A_6 (μs)
SHA30	0.4944	− 0.1283	0.0121	3.49	0.83	10.267
SHA70	1.6926	− 0.4226	0.0648	5.61	17.02	19.85

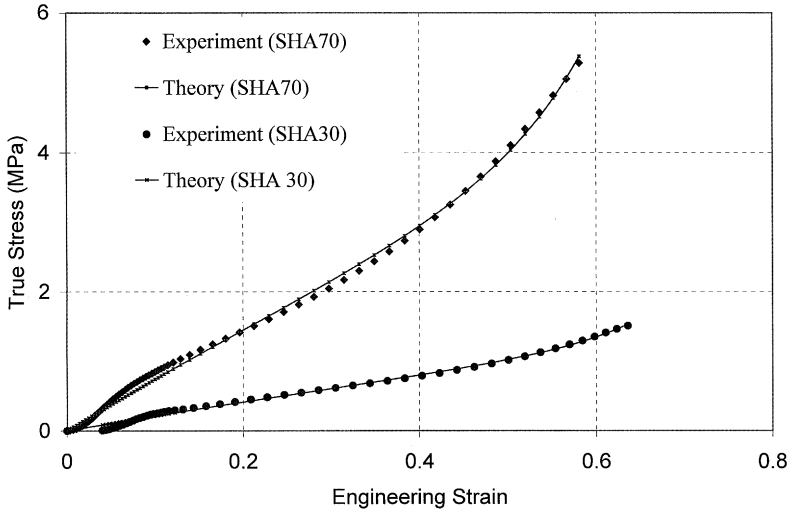

Fig. 1. Comparison between quasi-static experimental data and proposed model.

3. Viscoelasticity

A primary characteristic of viscoelastic materials is the effect of previous deformation; the stress state depends on the strain and/or strain rate histories. The constitutive relationship for a homogeneous, isotropic and incompressible material can be expressed in the following form [8–11]:

$$\sigma^{\mathrm{v}} = -p^{\mathrm{v}} + \mathbf{F}(t)\cdot \overset{t}{\underset{\tau=-\infty}{\Omega}} \{\mathbf{C}(\tau)\}\cdot \mathbf{F}^{\mathrm{T}}(t), \tag{9}$$

where σ^{v} is the Cauchy stress tensor, p^{v} the pressure for a viscoelastic material, and Ω is a matrix functional which describes the effect of strain history on stress; this relationship is frame-independent [11]. Numerous approximations to represent the functional Ω have been proposed for solids and these are described in the work by Lockett [11] and more recently by others [4,12]. From these studies, a significant result was that relatively few parameters are needed to model finite strain viscoelastic material behaviour. A number of non-linear viscoelastic constitutive models were introduced in the monograph by Carreau et al. [12]. An area of focus with respect to viscoelastic models is to simplify the function Ω; for example, the BKZ model [9,10] and its applications [13].

Here, the functional Ω is assumed to have the following form

$$\overset{t}{\underset{\tau=-\infty}{\Omega}}\{\mathbf{C}(\tau)\} = \int_{-\infty}^{t} \phi(I_1, I_2) m(t-\tau)\dot{\mathbf{E}}(\tau)\,\mathrm{d}\tau, \tag{10}$$

where the strain rate is defined by

$$\dot{\mathbf{E}} = \tfrac{1}{2}(\dot{\mathbf{F}}^{\mathrm{T}}\cdot\mathbf{F} + \mathbf{F}^{\mathrm{T}}\cdot\dot{\mathbf{F}}) \tag{11}$$

and the relaxation function $m(t)$ decreases with t; in general, $m(t)$ is assumed to be an exponential series described by

$$m(t-\tau) = \sum_{i=1}^{N} \exp\left(-\frac{t-\tau}{\theta_i}\right), \tag{12}$$

where θ_i is the relaxation time.

N was assigned a value of 2 by several researchers [14–16], who designated the label "ZWT model" to their formulation, whereby one relaxation time is used to describe behaviour at low strain rates (10^{-4}–$10^{-1}\,\mathrm{s}^{-1}$) and another to characterise behaviour at high strain rates (10^{2}–$10^{3}\,\mathrm{s}^{-1}$). In the version proposed by Osaki et al. [17] a value of $N = 5$ was assumed, while Wagner [18] selected $N = 8$. It has been reported [19] that the relaxation times depend on the micro-structure of the materials. Motion within the microstructure, which determines the relaxation time, is activated by a corresponding loading rate. From the viewpoint of macro-mechanical behaviour of materials, the relaxation time recorded in a test depends on the loading time or loading rate. For many polymeric materials deformed at strain rates generated by conventional SHPB devices, mechanical response can be adequately described by a single relaxation time [14–16]. In general, a good material model would not require an excessive number of parameters to describe the essential features of the associated experimental phenomenon. Hence, in this study, only one relaxation time is used; i.e. $N = 1$ in Eq. (12).

Based on the motivation to minimise the number of parameters, the function ϕ in Eq. (10) is assumed to be

$$\phi(\tau) = A_4 + A_5(I_2'(\tau) - 3), \tag{13}$$

where I_2' is the second invariant of $\mathbf{C}(\tau)$. (It can be shown that I_2' in the viscoelastic case is equal to I_2 in the hyperelastic case.) The starting point for time is taken to be the instant at which loading commences and it is assumed that the effect of deformation history for $\tau < 0$ on the stress at time $t > 0$ is ignored. Thus, the period of deformation history which is considered to affect the stress response — i.e. the limits of integration in the second term on the right-hand side of Eq. (10) — becomes $[0, t]$ rather than $(-\infty, t]$. Substituting Eqs. (13) and (12) with $N = 1$ into Eq. (10) results in the following proposed integral approximation for Ω,

$$\overset{t}{\underset{\tau=-\infty}{\Omega}}\{\mathbf{C}(\tau)\} = \int_{0}^{t} [A_4 + A_5(I_2 - 3)]\exp\left(-\frac{t-\tau}{A_6}\right)\dot{\mathbf{E}}(\tau)\,\mathrm{d}\tau. \tag{14}$$

Substitution of Eq. (14) into Eq. (9) yields a frame-independent finite strain viscoelastic model for incompressible materials.

$$\sigma^{v} = -p^{v}\mathbf{I} + \mathbf{F}(t)\cdot\left[\int_0^t [A_4 + A_5(I_2 - 3)]\exp\left(-\frac{t-\tau}{A_6}\right)\dot{\mathbf{E}}(\tau)\,d\tau\right]\cdot[\mathbf{F}(t)]^{T}. \tag{15}$$

4. Visco-hyperelasticity

It is proposed that visco-hyperelastic behaviour arises from a combination of hyperelasticity and viscoelasticity, whereby the total stress is the sum of these individual components, i.e. $\sigma = \sigma^{e} + \sigma^{v}$, where σ^{e} and σ^{v} are defined by Eqs. (1) and (15), respectively. This assumption means that the stress–strain behaviour of rubber-like materials can be separated into a quasi-static hyperelastic component (σ^{e}) and a rate-dependent response (σ^{v}) governed by Eq. (15). Consequently, summation of Eqs. (1) and (15) yields:

$$\sigma = -p\mathbf{I} + \alpha_1\mathbf{B} + \alpha_2\mathbf{B}\cdot\mathbf{B} + \mathbf{F}\cdot\left(\int_0^t (A_4 + A_5 I_2)\exp\left(-\frac{t-\tau}{A_6}\right)\dot{\mathbf{E}}(\tau)\,d\tau\right)\cdot\mathbf{F}^{T}, \tag{16}$$

where $p(=p^{e}+p^{v})$ is the total pressure comprising static and viscoelastic components and α_1 and α_2 are defined by Eq. (6). A_4, A_5 and A_6 are material parameters which characterise the viscoelastic response under high strain rates and are determined from tests involving dynamic uniaxial loading of specimens. Substitution of the strain rate $\dot{E}_{11} = \lambda\dot{\lambda}$ into Eq. (16) yields the stress-deformation relation in the direction of loading:

$$\sigma_{11} = -p^{v} + \sigma^{e}_{11} + \lambda^2\int_0^t \lambda[A_4 + A_5(I_2 - 3)]\exp\left(-\frac{t-\tau}{A_6}\right)\dot{\lambda}\,d\tau, \tag{17}$$

where σ^{e}_{11} is described by Eq. (8) and p^{v} is determined from the condition that the transverse stress $\sigma_{22} = 0$, and can be written as

$$p^{v} = -\tfrac{1}{2}\lambda^{-1}\left(\int_0^t \lambda^{-2}[A_4 + A_5(I_2 - 3)]\exp\left(-\frac{t-\tau}{A_6}\right)\dot{\lambda}\,d\tau\right). \tag{18}$$

Substitution of the preceding expression for p^{v} into Eq. (16) yields the relationship between stress and deformation in the direction of loading.

$$\sigma_{11} = \sigma^{e}_{11} + \lambda^2\int_0^t \lambda[A_4 + A_5(I_2 - 3)]\exp\left(-\frac{t-\tau}{A_6}\right)\dot{\lambda}\,d\tau + \tfrac{1}{2}\lambda^{-1}\int_0^t \lambda^{-2}[A_4 + A_5(I_2 - 3)]\exp\left(-\frac{t-\tau}{A_6}\right)\dot{\lambda}\,d\tau, \tag{19}$$

where the rate of stretching is equal to the engineering strain rate; i.e. $\dot{\lambda} = \dot{\varepsilon}_{11}$. Dynamic uniaxial compression tests were conducted on SHA30 and SHA70 rubber specimens using a Split Hopkinson Pressure Bar to obtain stress–strain data. For SHA30 rubber, data corresponding to average

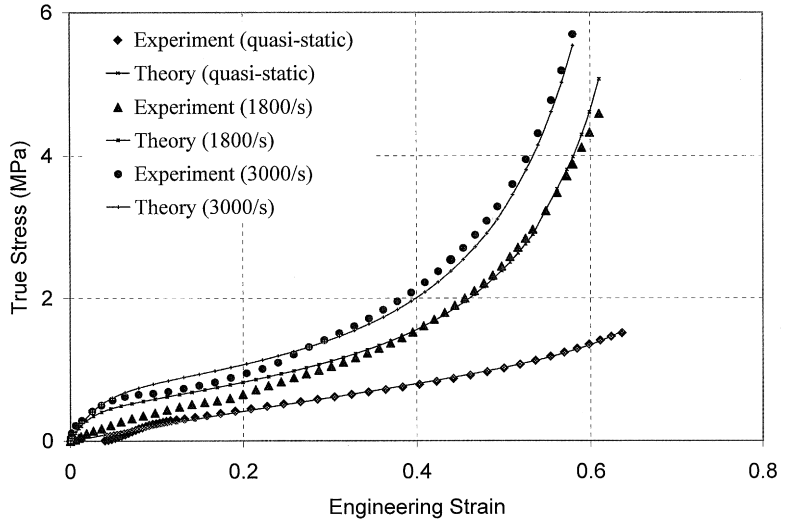

Fig. 2. Comparison between theoretical curves and experimental data for SHA30 rubber.

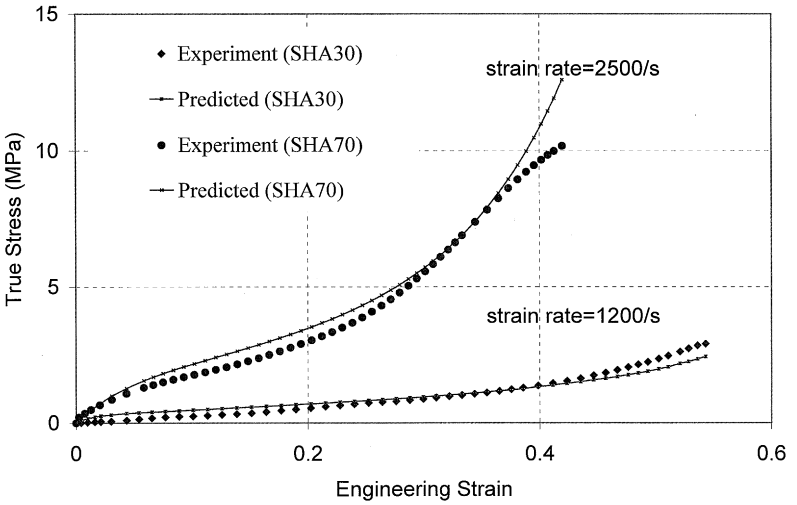

Fig. 3. Comparison between predicted and experimental response at high strain rates.

strain rates of 1800 and 3000 s^{-1} were used to determine the parameters A_4, A_5 and A_6 via a least-squares fit. The values of these parameters are listed in Table 1 and a comparison between the fitted curves and test data is shown in Fig. 2. Substitution of the values of A_i into Eq. (19) facilitates prediction of stress–strain response at high strain rates. Validity of the proposed model is confirmed by conducting a dynamic test at a strain rate of 1200 s^{-1} and comparing the experimental data with the curve generated by the constitutive equation. Fig. 3 shows very good correlation between prediction and experiment.

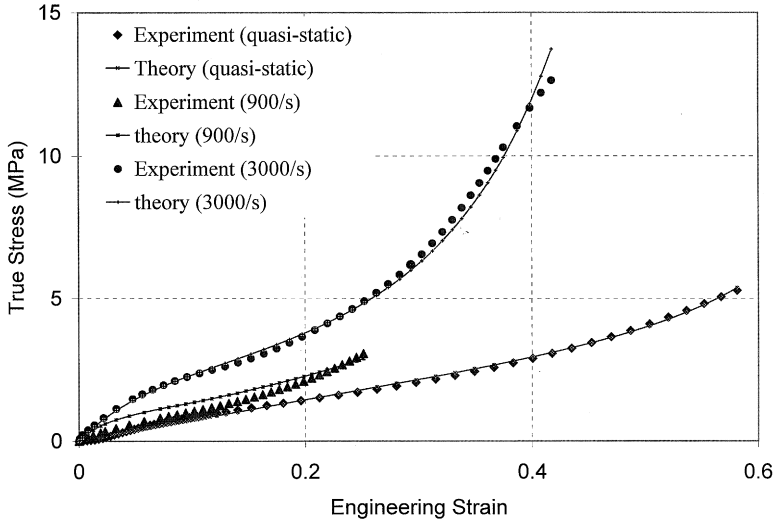

Fig. 4. Comparison between theoretical curves and experimental data for SHA70 rubber.

To further substantiate applicability of the analysis to rubber material of other hardnesses, the same procedure was adopted for SHA70 rubber. Two experimental stress–strain curves from SHPB tests, corresponding to average strain rates of 900 and 3000 s^{-1} were used to evaluate the parameters A_4, A_5 and A_6 (see Table 1). A comparison of the theoretical curves with test data is shown in Fig. 4. Again, confirmation of the proposed constitutive relationship is provided by its correlation with experiments at a strain rate 2500 s^{-1} (Fig. 3). Figs. 2–4 show that the proposed model is well-suited for the description of visco-hyperelastic behaviour of rubber-like materials loaded at high strain rates.

5. Verification of proposed model via numerical modelling and impact testing

To demonstrate the validity of the proposed visco-hyperelastic model, it is incorporated into a finite-element code and used to simulate the three-dimensional response of different grades of rubber subjected to impact by an essentially rigid striker. Computational predictions are compared with experiments involving the dropping of an impactor onto rubber pads.

The experimental arrangement is shown in Fig. 5. A rubber pad is struck by an impactor in the form of a hemispherically tipped cylinder of 30 mm diameter. This impactor is made of aluminium, and is allowed to fall freely through a tube, which serves as a guide to ensure the striker experiences normal impact against the rubber specimen. The thickness of SHA-30 rubber specimens is 1.0 and 1.5 mm for SHA-70 specimens. They are placed on a 5 mm thick steel plate and the impact velocity of the impactor is measured by the interruption of a pair of laser beams sited in its path. The impact force is determined from a load-cell on which the steel plate supporting the specimen rests, while an accelerometer mounted on the impactor measures its deceleration.

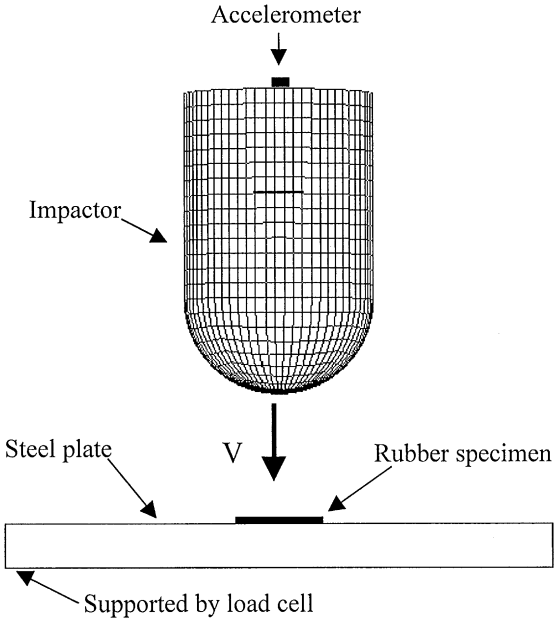

Fig. 5. Impact test arrangement and finite element model.

The well-known finite element code, DYNA3D, developed by the Lawrence Livermore National Laboratory, is used to simulate the experiments described. Firstly, the proposed hyper-viscoelastic model defined by Eq. (16), is incorporated as a material model subroutine. In the simulations, the impactor is assumed to be rigid, as its deformation relative to that of the rubber is negligible. From experiments, the impact velocities were $2.250\,\mathrm{m\,s^{-1}}$ for SHA-30 rubber and $2.514\,\mathrm{m\,s^{-1}}$ for SHA-70 rubber, respectively; these values were used in the simulations and comparisons with test data are shown in Figs. 6 and 7. Fig. 6 is a comparison of acceleration and Fig. 7 compares the force transmitted through the steel plate to the load cell beneath. As the specimens experience a large range of strain rates during testing, it is difficult to encapsulate the entire response exactly using a single relaxation time (this is discussed in the next section). This, coupled with experimental variability, accounts for discrepancies between the simulation results and recorded data in Figs. 6 and 7. However, there is sufficient agreement to substantiate that the proposed hyper-viscoelastic model based on uniaxial test data is able to yield a reasonable description of a situation where deformation is not uniform.

6. Discussion of the viscoelastic model

In essence, Eq. (14) describes viscoelastic behaviour which is analogous to the generalised Maxwell model shown in Fig. 8, where the non-linear tangent modulus E of the spring, as well as the dashpot viscosity η, depends on the strain ($\eta/E = A_6$ is a constant which defines the relaxation time of the model). It is assumed that the strain rate $\dot{\mathbf{E}}$ in Eq. (14) can be considered to be the sum of

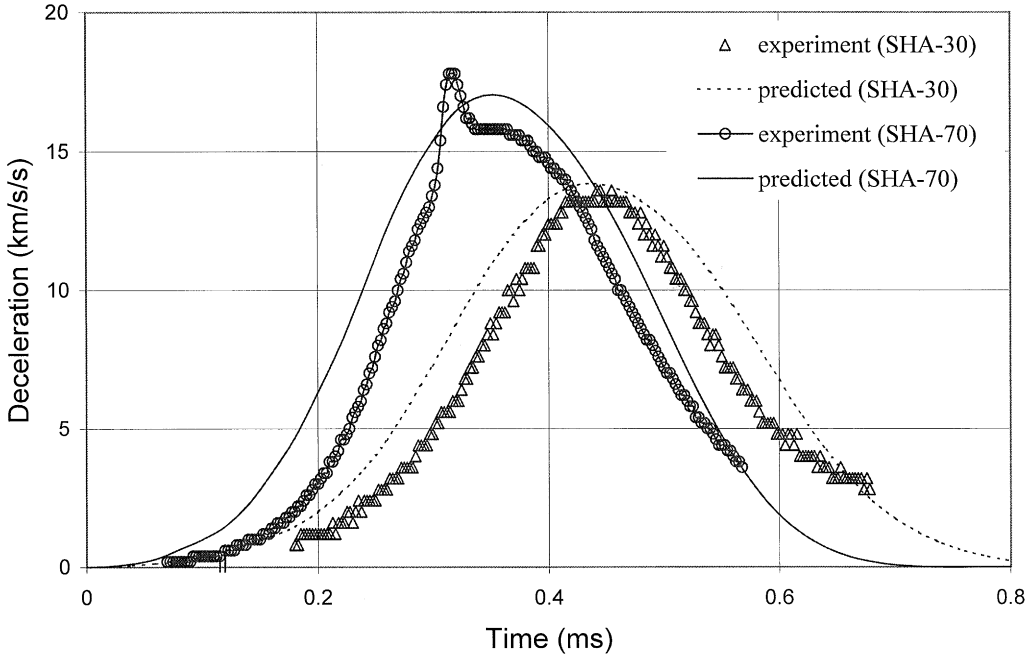

Fig. 6. Comparison between experimental and predicted impactor deceleration.

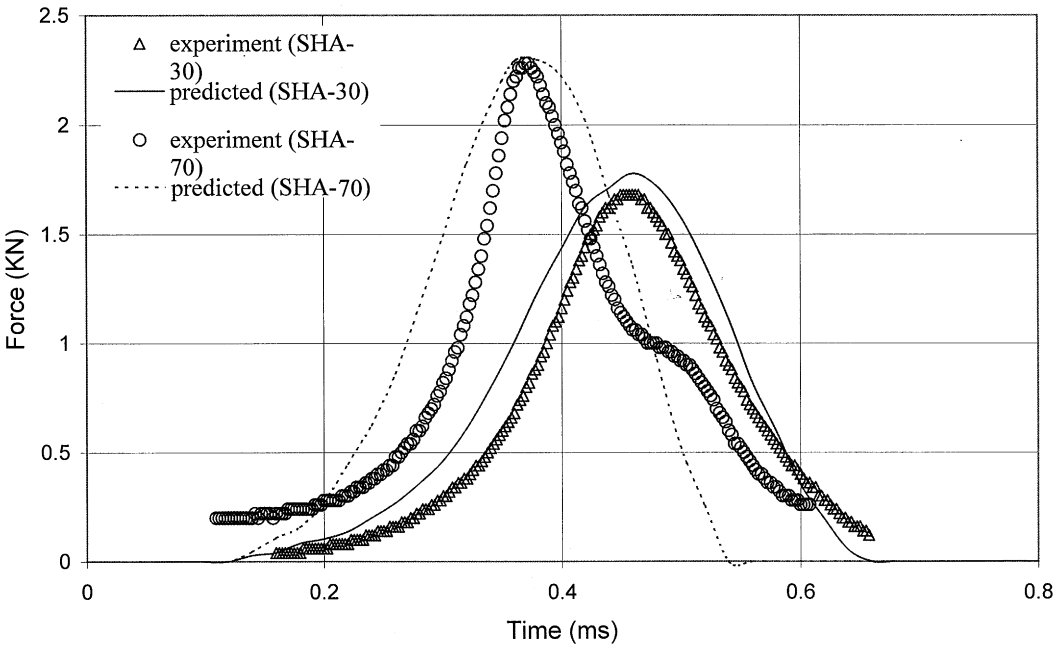

Fig. 7. Comparison between experimental and predicted impact force.

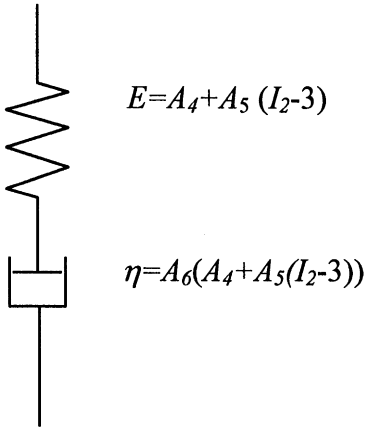

Fig. 8. Generalised Maxwell model.

the strain rates of the spring and dashpot elements $\dot{\mathbf{E}}_E$ and $\dot{\mathbf{E}}_\eta$ of the generalised Maxwell model. When $A_5 = 0$, or for situations of infinitesimal strain where $I_2 - 3$ is much less than 1, the model degenerates to the linear Maxwell model. Therefore, A_5 is the parameter which describes the effect of strain on the tangent modulus of the non-linear spring and A_4 is the linear component of the spring modulus.

Rate sensitivity is embodied in the relaxation time A_6. In a viscoelastic model, the number of relaxation time constants is an important parameter, as it determines the value of N in Eq. (12). The larger N is, the more closely the model can be made to fit experimental data; however, this implies that the number of parameters which need to be determined is correspondingly greater. The objective of the present study is to formulate a material model which minimises the number of such parameters without significantly compromising correlation with actual behaviour. To achieve this, how a relaxation time constant affects material model behaviour is examined. To understand the relationship between strain rate and the relaxation time constant of a generalised Maxwell model, its governing equation (14), can be written in the form of a non-dimensional relationship:

$$\mathbf{S} = \int_0^s [1 + a(I_2 - 3)]\exp[-(s-\beta)]\dot{\mathbf{D}}(\beta)\,\mathrm{d}\beta, \tag{20}$$

where $\mathbf{S} = \mathbf{\Omega}/A_4$ is the non-dimensionalised stress, $\dot{\mathbf{D}} = A_6\dot{\mathbf{E}}$ the non-dimensionalised strain rate and $a = A_5/A_4$, $s = t/A_6$, $\beta = \tau/A_6$.

Consider a situation of uniaxial loading which induces a constant rate of stretch ($\dot{\lambda} = \text{constant}$). The non-dimensional stretch rate is $\dot{\zeta} = A_6\dot{\lambda}$. The stretch $\lambda = s\dot{\zeta}$ is then substituted into Eq. (3) to determine $\mathbf{F}$; and the strain rate can be determined from Eq. (11). The effect of the stretch rate $\dot{\zeta}$ on the resulting stress–strain curves is shown in Fig. 9, which indicates that the regime of greatest rate sensitivity corresponds to non-dimensional strain rates ranging from 10^{-2} to 10^{0}. For non-dimensional strain rates $\dot{\zeta}$ less than 10^{-2}, the magnitude of the stress $\mathbf{S}$ is small. When $\dot{\zeta} > 10^{0}$, the response is essentially defined by the non-linear spring. Consequently, the proposed model encapsulates the effects of both strain rate and strain history on stress most aptly when

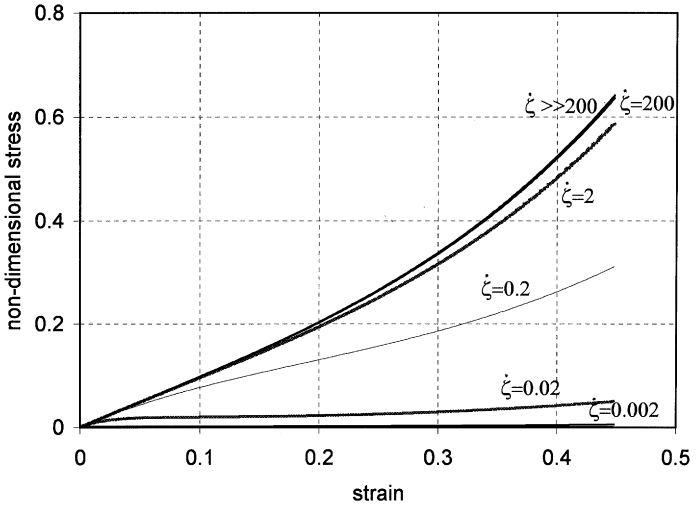

Fig. 9. Effect of strain rate on stress; Eq. (31), $n = 1$.

$10^{-2} < \dot{\zeta} < 10^{0}$. This conclusion applies to compression as well as tension; i.e. the range of rate sensitivity captured by the present model is $10^{-2} < |\dot{\zeta}| < 10^{0}$, the implication being that one relaxation time constant can only describe viscoelastic response for changes of strain rate within two orders of magnitude. This conclusion differs somewhat from that presented by Chu et al. [20], who examined a linear Maxwell model and proposed that a relaxation time has an "effective influence domain" of about 4.5 orders of magnitude. The difference between the present analysis and their conclusion arises from the non-linear stress–strain relationship of the viscoelastic model considered in this paper. Based on current findings, variation in strain rate of more than two orders of magnitude requires two or more relaxation times. It is recognised that several relaxation time constants are needed to describe the full range of mechanical behaviour of a polymer, and that each relaxation time corresponds to one mode of micro-structural motion. Based on Fig. 9 and bearing in mind that $\dot{\zeta} = A_6\dot{\lambda}$ for a constant rate of stretching, it can be seen that loading which produces a stretch rate of $\dot{\lambda}$ will activate the mode of micro-structural motion which corresponds to a relaxation time A_6 in the range of $10^{-2}/\dot{\lambda}$ to $10^{0}/\dot{\lambda}$.

Thus, the relaxation time constant determined by the relatively high strain rate tests in this investigation ($\dot{\lambda} \sim 10^{3}\ \mathrm{s}^{-1}$) is associated only with the short-term response of rubber, in which the relaxation time is about 10^{-5} s. The longer-term response corresponding to low strain rates should be characterised by larger relaxation times; this has not been investigated in the present study. However, in general, stress increases with strain rate for rubber. From the dynamic stress–strain curves obtained experimentally, it appears reasonable to conclude that the rate effect at low strain rates is not significant and hence can be ignored compared to its effect at high strain rates. This is because enhancement of stress at high strain rates is far more pronounced. Therefore, only one relaxation time is used to describe the rate sensitivity of rubber in the present study. Nevertheless, it has been demonstrated that the proposed constitutive model, which only requires determination of a few parameters, is able to describe the observed behaviour rather well. However, it is not expected that the present equation would be suitable for defining low strain rate response ($\dot{\lambda} < 10^{1}\ \mathrm{s}^{-1}$). For

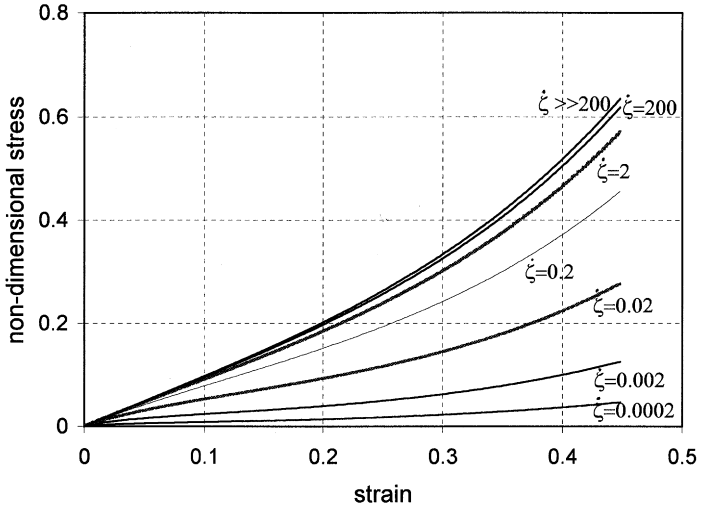

Fig. 10. Effect of strain rate on stress; Eq. (31), $n = 2$.

example, the response at strain rates of the order of $10^0\ s^{-1}$ should be described by a relaxation time with an order of magnitude of 10^{-2}–10^0 s. It has been assumed in the present investigation that the low strain rate behaviour of rubber is essentially the same as its static response; the experimental results confirm that such an assumption does not generate significant error.

The proposed model is further examined to see if it is possible to extend its coverage of rate-sensitive material response without increasing the number of parameters to be determined. Consider again the model shown in Fig. 8, but with the dashpot viscosity now defined by $\eta = A_6^{1/n}[A_4 + A_5(I_2 - 3)]t^{1-1/n}/n$, while the tangent modulus E remains unchanged. The stress-time response of this generalised Maxwell model now becomes

$$\sigma = \int_0^t [A_4 + A_5(I_2 - 3)]\exp\left(-\frac{t^{1/n} - \tau^{1/n}}{A_6^{1/n}} \right)\dot{\mathbf{E}}(\tau)\, \mathrm{d}\tau. \tag{21}$$

In non-dimensional terms:

$$\mathbf{S} = \int_0^s [1 + a(I_2 - 3)]\exp[-(s^{1/n} - \beta^{1/n})]\dot{\mathbf{D}}(\beta)\, \mathrm{d}\beta, \tag{22}$$

where the definitions of $\mathbf{S}$, a, s, β and $\dot{\mathbf{D}}$ remain the same as that in Eq. (20). As with the preceding analysis, the case of deformation at a constant stretch rate ($\dot{\lambda} = \text{constant}$) by uniaxial loading is examined, whereby the non-dimensional stretch rate is $\dot{\zeta} = A_6\dot{\lambda}$. By assuming $n = 2$ in Eq. (22), the effect of non-dimensional stretch rate $\dot{\zeta}$ on the stress–strain relationship is shown in Fig. 10. It can be seen that the range of rate sensitivity has expanded to 10^{-4}–10^0, implying that a single relaxation time constant can now describe rate-dependent response spanning four orders of magnitude. However, Fig. 10 also shows that Eq. (22) yields less pronounced rate sensitivity

compared to Eq. (20). This arises from the fact that the stress response of the dashpot corresponding to Eq. (20) is $\sigma_\eta = A_6[A_4 + A_5(I_2 - 3)]\dot{\mathbf{E}}$, which is proportional to the strain rate $\dot{\mathbf{E}}$, whereas the response associated with Eq. (22), with $n = 2$ is

$$\sigma_\eta = \tfrac{1}{2} A_6^{1/2}[A_4 + A_5(I_2 - 3)]t^{1/2}\dot{\mathbf{E}}. \tag{23}$$

The stress now has an order of magnitude of $f(\mathbf{E}) \cdot \dot{\mathbf{E}}^{1/2}$ and is proportional to the square root of the strain rate; i.e. $\dot{\mathbf{E}}^{1/2}$. This analysis shows that a larger value of n in Eq. (22) results in the capacity to describe a larger range of strain rates, but the degree of rate sensitivity decreases with n. It is also noted that the model described by Eq. (20) is a special case of that described by Eq. (22); the former has a value of $n = 1$.

7. Conclusions

By employing a fundamental approach to the formulation of constitutive relationships, a new constitutive equation is proposed to describe three-dimensional visco-hyperelastic large deformation behaviour of incompressible rubber-like materials under high strain rates. Static response is accommodated by a component comprising a hyperelastic relationship based on an elastic strain energy potential. It is found that a three-term truncated series for this potential adequately describes the hyperelasticity of the material. Another component in the equation, a generalised Maxwell model, is introduced to characterise viscoelastic response under high strain rates. The total expression corresponds to a hyperelastic solid in parallel with a generalised Maxwell model, thus characterising not only hyperelasticity but also strain rate and strain history dependent viscoelasticity. Stress–strain curves predicted by the model for two kinds of rubber are compared with the experimental data derived from SHPB tests. The comparisons show that the proposed model is well-suited for the description of visco-hyperelastic behaviour of rubber-like materials loaded at high strain rates. In addition, the proposed material model is incorporated into a finite element code (DYNA3D) and employed in the simulation of three-dimensional dynamic (impact) loading of rubber. The numerical results exhibit good agreement with experimental data, demonstrating that the model is suitable for prediction of visco-hyperelastic behaviour in situations different from that used to determine its parameters. As the proposed stress–strain relationship is based on well-established theoretical approaches to constitutive modelling, it is able to describe three-dimensional response of rubber-like materials, even though the parameters in the model are determined from tests involving uniaxial loading.

The assumption of only one relaxation time constant A_6, derived from experimental tests at relatively high strain rates ($\dot{\varepsilon} \sim 10^3\ \mathrm{s}^{-1}$), limits its application to strain rates of that order. A study was made of the range of strain rates which can be described by the generalised Maxwell model used in the analysis. This resulted in the formulation of a more generalised form of the Maxwell model, whereby the relationship between stress and strain rate associated with the dashpot is assumed to be proportional to the nth root of the strain rate, $\sigma_\eta \sim \dot{E}^{1/n}$. Such a model can be used to capture a larger range of rate-sensitive behaviour.

References

[1] Johnson AR, Quigley CJ. A viscohyperelastic Maxwell model for rubber viscoelasticity. Rubber Chem Technol 1992;65:137–53.
[2] Johnson AR, Quigley CJ, Freese CE. A viscoplastic finite element model for rubber. Comput Methods Appl Mech Eng 1995;127:163–80.
[3] Ward IM. Mechanical properties of solid polymers. New York: Wiley, 1983.
[4] Drozdov AD, Kolmanovskii VB. Stability in viscoelasticity. Amsterdam: North-Holland, 1994.
[5] Rao S, Shim VPW, Quah SE. Dynamic mechanical properties of polyurethane elastomers using a nonmetallic Hopkinson bar. J Appl Polym Sci 1997;66:619–31.
[6] Rivlin RS. Proceedings of First Symposium on Naval Structural Mechanics, 1960. p. 169–98.
[7] Brown RP. Physical testing of rubber, 3rd ed. London: Chapman & Hall, 1996.
[8] Truesdell C, Noll W. The non-linear field theories of mechanics. In: Flugge S, editor. Handbuch der Physik. Berlin: Springer, 1965.
[9] Bernstein B, Kearsley A, Zapas LJ. Trans Soc Rheol 1963;7:391–410.
[10] Bernstein B, Kearsley A, Zapas LJ. A study of stress relaxation with finite strain. Rubber Chem Technol 1965;38:76–89.
[11] Lockett FJ. Non-linear viscoelastic solids. New York: Academic Press Inc. Ltd., 1972.
[12] Carreau PJ, De Kee DCR, Chhabra RP. Rheology of polymeric systems: principles and applications. Hanser Publishers, 1997.
[13] Tanner RI. From A to (BK)Z in constitutive relations. J Rheol 1988;32:673–702.
[14] Tang ZP, Tian LQ, Chu CH, Wang LL. Mechanical behaviour of epoxy resin under high strain rate. Proceedings of Second National Conference on Explosive Mechanics, 1981. p.4–1–2.
[15] Wang LL, Yang LM. A class of non-linear viscoelastic constitutive relation of solid polymeric materials. In: Wang LL, Yu TX, Li YC. editors. The progress in impact dynamics. 1992. p. 88–116.
[16] Wang LL, Huang D, Gan S. Non-linear viscoelastic constitutive relations and non-linear wave propagation for polymers at high strain rates. In: Kawata K, Shioiri J, editors. Constitutive relation in high/very high strain rates. IUTAM Symposium Noda/Japan, 1995. p. 137–146.
[17] Osaki K, Ohta S, Fukuda M, Kulata M. J Polym Sci 1976;14:1701–15.
[18] Wagner MH. Rheol Acta 1979;18:33–50.
[19] Ferry JD. Viscoelastic properties of polymers. New York: Wiley, 1980.
[20] Chu CH, Wang LL, Xu DB. A non-linear thermo-viscoelastic constitutive equation for thermoset plastics at high strain rates. In: Chien Wei-Zeng, editor. Proceedings of the International Conference on Non-linear Mechanics, October 28–31, 1985, Shanghai, China, Beijing: Science Press, 1985. p. 92–7.